increased expression of *CDKN1C* might reside on an unexamined region(s) such as promoter or enhancer sequences. In this regard, while case 3 showed IMAGe syndrome-compatible clinical features such as IUGR, metaphyseal dysplasia, adrenal hypoplasia and genital abnormalities, case 3 lacked slender bones and had arachnodactyly, in contrast to *CDKN1C*-mutation-positive cases 1 and 2. Such mild but discernible phenotypic variation might reflect the genetic heterogeneity. This matter might be clarified in the future by extensive studies such as exome or whole-genome sequencing. In particular, when such *CDKN1C*-mutation-negative patients with IMAGe syndrome-compatible phenotype have been accumulated, a novel gene(s) mutated in such patients may be identified. In this regard, if such a gene(s) exist, it is predicted to reside in the signal transduction pathway involving *CDKN1C*.

Relevance of CDKN1C mutations to atypical IMAGe syndrome and SRS

CDKN1C mutations have also been identified in atypical IMAGe syndrome and SRS (Fig. 1a). Hamajima *et al.* revealed a maternally inherited p.Ile272Ser mutation in three siblings (two males and one female) who manifested IUGR and adrenal insufficiency, and male genital abnormalities, but had no skeletal lesion.[22] Similarly, Brioude *et al.* found a maternally transmitted p.Arg279Leu mutation in six relatives (all females) from a four-generation family who satisfied the SRS diagnostic criteria,[23,24] after studying 97 SRS patients without known causes of SRS, that is, hypomethylation (epimutation) of the *H19*-DMR, duplication of the ICR2 and maternal uniparental disomy for chromosome 7 (upd(7)mat).[24] Notably, although both mutations had no significant effect on a cell cycle, they were associated with increased protein stability that appears to be consistent with the gain-of-function effects.[22,24] Such increased stability was also found for IMAGe-associated missense mutant proteins,[22] and an altered cell cycle with a significantly higher proportion of cells in the G1 phase was shown for an IMAGe-associated p.Arg279Pro mutation.[24] It is possible therefore that relatively severe *CDKN1C* gain-of-function effects lead to IMAGe syndrome and relatively mild *CDKN1C* gain-of-function effects result in SRS, with intermediate *CDKN1C* gain-of-function effects being associated with atypical IMAGe syndrome.[24]

Thus, it would not be surprising that cases 1–3 also met the SRS diagnostic criteria (Table 3).[23,24] Indeed, cases 1–3, as well as *CDKN1C*-mutation-positive SRS patients,[24] exhibited pre- and post-natal growth failure with relative macrocephaly and frequently manifested feeding difficulties and/or low body mass index (BMI) at two years of age. However, while relative macrocephaly is usually obvious at birth in SRS patients with *H19*-DMR epimutations and upd(7)mat,[21,23,25] it is more obvious at 2 years of age than at birth in *CDKN1C*-mutation-positive SRS patients.[24] Furthermore, *CDKN1C*-mutation-positive SRS patients are free from body asymmetry,[24] as are typical and atypical IMAGe syndrome patients described in this study and in the previous studies.[1–4,7,22] Thus, SRS caused by *CDKN1C* mutations may be characterized by clinically discernible macrocephaly at two years of age and lack of body asymmetry.

Table 3. Silver–Russell syndrome phenotypes in cases 1–3 and in affected relatives reported by Brioude *et al.*

	Case 1	Case 2	Case 3	Brioude *et al.**
Mandatory criteria				
IUGR†	Yes	Yes	Yes	4/4
Scoring system criteria				
Postnatal short stature (≤−2 SDS)	Yes	Yes	Yes	4/4
Relative macrocephaly‡	Yes	Yes	Yes	4/4§
Prominent forehead during early childhood	Yes	Yes	Yes	4/4
Body asymmetry	No	No	No	0/4
Feeding difficulties during early childhood and/or low BMI (<−2·0 SDS) around 2 years of age	Yes	Yes	Unknown	3/4 (1/4 & 2/4)¶

IUGR, Intrauterine growth retardation; SDS, standard deviation score; and BMI, body mass index.
The SRS diagnostic criteria proposed by Netchine *et al.*[23] and Brioude *et al.*[24] (low BMI around 2 years of age is included in Brioude *et al.*, but not in Netchine *et al.*): The diagnosis of SRS is made, when mandatory criteria plus at least three of the five scoring system criteria are observed. For detailed clinical features in cases 1–3, see Table 1.
*While six relatives were found to have *CDKN1C* mutation, detailed clinical features have been obtained in four mutation-positive relatives.[24]
†Birth length and/or birth weight ≤−2 SDS for gestational age.
‡SDS for birth length or birth weight minus SDS for birth occipitofrontal circumference ≤−1·5.
§Relative macrocephaly is more obvious at 2 years of age (4/4) than at birth (2/4).
¶One patient is positive for feeding difficulties, and other two patients are positive for low BMI.

Conclusion

In summary, we studied three patients with IMAGe syndrome. The results provide implications for phenotypic spectrum, underlying factor(s) in the development of each phenotype and genetic heterogeneity in IMAGe syndrome, as well as a phenotypic overlap between IMAGe syndrome and SRS. Further studies will permit to elucidate such matters.

Funding

This study was supported in part by Grants-in-Aid for Scientific Research (A) (25253023) and for Scientific Research on Innovative Areas (22132004-A01) from the Ministry of Education, Culture, Sports, Science and Technology, by Grant for Research on Intractable Diseases from the Ministry of Health, Labor and Welfare (H24-048), and by Grants from National Center for Child Health and Development (23A-1, 24-7 and 25-10).

Declaration of interest

The authors have nothing to declare.

References

1 Vilain, E., Le Merrer, M., Lecointre, C. *et al.* (1999) IMAGe, a new clinical association of intrauterine growth retardation, metaphyseal dysplasia, adrenal hypoplasia congenita, and genital anomalies. *Journal of Clinical Endocrinology and Metabolism*, **84**, 4335–4340.

2 Balasubramanian, M., Sprigg, A. & Johnson, D.S. (2010) IMAGe syndrome: case report with a previously unreported feature and review of published literature. *American Journal of Medical Genetics A*, **152A**, 3138–3142.

3 Bergadá, I., Del Rey, G., Lapunzina, P. *et al.* (2005) Familial occurrence of the IMAGe association: additional clinical variants and a proposed mode of inheritance. *Journal of Clinical Endocrinology and Metabolism*, **90**, 3186–3190.

4 Arboleda, V.A., Lee, H., Parnaik, R. *et al.* (2012) Mutations in the PCNA-binding domain of CDKN1C cause IMAGe syndrome. *Nature Genetics*, **44**, 788–792.

5 Demars, J. & Gicquel, C. (2012) Epigenetic and genetic disturbance of the imprinted 11p15 region in Beckwith-Wiedemann and Silver-Russell syndromes. *Clinical Genetics*, **81**, 350–361.

6 Lee, M.-H., Reynisdottir, I. & Massague, J. (1995) Cloning of p57(KIP2), a cyclin-dependent kinase inhibitor with unique domain structure and tissue distribution. *Genes and Development*, **9**, 639–649.

7 Amano, N., Naoaki, H., Ishii, T. *et al.* (2008) Radiological evolution in IMAGe association: a case report. *American Journal of Medical Genetics A*, **146A**, 2130–2133.

8 El-Khairi, R., Martinez-Aguayo, A., Ferraz-de-Souza, B. *et al.* (2011) Role of DAX-1 (NR0B1) and steroidogenic factor-1 (NR5A1) in human adrenal function. *Endocrine Development*, **20**, 38–46.

9 Meimaridou, E., Hughes, C.R., Kowalczyk, J. *et al.* (2013) Familial glucocorticoid deficiency: new genes and mechanisms. *Molecular and Cellular Endocrinology*, **371**, 195–200.

10 Matsuoka, S., Thompson, J.S., Edwards, M.C. *et al.* (1996) Imprinting of the gene encoding a human cyclin-dependent kinase inhibitor, p57KIP2, on chromosome 11p15. *Proceedings of the National Academy of Sciences of the USA*, **93**, 3026–3030.

11 Yamazawa, K., Kagami, M., Nagai, T. *et al.* (2008) Molecular and clinical findings and their correlations in Silver-Russell syndrome: implications for a positive role of IGF2 in growth determination and differential imprinting regulation of the IGF2-H19 domain in bodies and placentas. *Journal of Molecular Medicine*, **86**, 1171–1181.

12 Ulaner, G.A., Yang, Y., Hu, J.F. *et al.* (2003) CTCF binding at the insulin-like growth factor-II (IGF2)/H19 imprinting control region is insufficient to regulate IGF2/H19 expression in human tissues. *Endocrinology*, **144**, 4420–4426.

13 Zhang, P., Leigeois, N.J., Wong, C. *et al.* (1997) Altered cell differentiation and proliferation in mice lacking p57(KIP2) indicates a role in Beckwith-Wiedemann syndrome. *Nature*, **387**, 151–158.

14 Karaplis, A.C., Luz, A., Glowacki, J. *et al.* (1994) Lethal skeletal dysplasia from targeted disruption of the parathyroid hormone-related peptide gene. *Genes & Development*, **8**, 277–289.

15 MacLean, H.E., Guo, J., Knight, M.C. *et al.* (2004) The cyclin-dependent kinase inhibitor p57(Kip2) mediates proliferative actions of PTHrP in chondrocytes. *Journal of Clinical Investigation*, **113**, 1334–1343.

16 Stewart, P.M. & Krone, N.P. (2011) The adrenal cortex. In: S. Melmed, K.S. Polonsky, P.R. Larsen, H.N. Kronenberg eds. Williams Textbook of Endocrinology, 12th edn. Elsevier, Saunders, 479–577.

17 Lienhardt, A., Mas, J.C., Kalifa, G. *et al.* (2002) IMAGe association: additional clinical features and evidence for recessive autosomal inheritance. *Hormone Research*, **57**(Suppl 2), 71–78.

18 Pedreira, C.C., Savarirayan, R. & Zacharin, M.R. (2004) IMAGe syndrome: a complex disorder affecting growth, adrenal and gonadal function, and skeletal development. *Journal of Pediatrics*, **144**, 274–277.

19 Ko, J.M., Lee, J.H., Kim, G.H. *et al.* (2007) A case of a Korean newborn with IMAGe association presenting with hyperpigmented skin at birth. *European Journal of Pediatrics*, **166**, 879–880.

20 Fowden, A.L., Sibley, C., Reik, W. *et al.* (2006) Imprinted genes, placental development and fetal growth. *Hormone Research*, **65** (Suppl 3), 50–58.

21 Wakeling, E.L., Amero, S.A., Alders, M. *et al.* (2010) Epigenotype-phenotype correlations in Silver-Russell syndrome. *Journal of Medical Genetics*, **47**, 760–768.

22 Hamajima, N., Johmura, Y., Suzuki, S. *et al.* (2013) Increased protein stability of CDKN1C causes a gain-of-function phenotype in patients with IMAGe syndrome. *PLoS ONE*, **8**, e75137.

23 Netchine, I., Rossignol, S., Dufourg, M.N. *et al.* (2007) 11p15 imprinting center region 1 loss of methylation is a common and specific cause of typical Russell-Silver syndrome: clinical scoring system and epigenetic-phenotypic correlations. *Journal of Clinical Endocrinology and Metabolism*, **92**, 3148–3154.

24 Brioude, F., Oliver-Petit, I., Blaise, A. *et al.* (2013) CDKN1C mutation affecting the PCNA-binding domain as a cause of familial Russell Silver syndrome. *Journal of Medical Genetics*, **50**, 823–830.

25 Fuke, T., Mizuno, S., Nagai, T. *et al.* (2013) Molecular and clinical studies in 138 Japanese patients with Silver-Russell syndrome. *PLoS ONE*, **8**, e60105.

26 Suwa, S., Tachibana, K., Maesaka, H. *et al.* (1992) Longitudinal standards for height and height velocity for Japanese children from birth to maturity. *Clinical Pediatric Endocrinology*, **1**, 5–14.

27 Inokuchi, M., Matsuo, N., Anzo, M. *et al.* (2007) Body mass index reference values (mean and SD) for Japanese children. *Acta Paediatrica*, **96**, 1674–1676.

28 Japan Public Health Association. (1996) Normal Biochemical Values in Japanese Children. Sanko Press, Tokyo, (in Japanese).

29 Matsuo, N. (1993) Skeletal and sexual maturation in Japanese children. *Clinical Pediatric Endocrinology*, **2**(Suppl), 1–4.

Supporting Information

Additional Supporting Information may be found in the online version of this article:

Table S1. Primers utilized in this study.

ORPHANET JOURNAL OF RARE DISEASES

RESEARCH Open Access

Japanese founder duplications/triplications involving *BHLHA9* are associated with split-hand/foot malformation with or without long bone deficiency and Gollop-Wolfgang complex

Eiko Nagata[1†], Hiroki Kano[2†], Fumiko Kato[1], Rie Yamaguchi[1], Shinichi Nakashima[1], Shinichiro Takayama[3], Rika Kosaki[4], Hidefumi Tonoki[5], Seiji Mizuno[6], Satoshi Watanabe[7], Koh-ichiro Yoshiura[7], Tomoki Kosho[8], Tomonobu Hasegawa[9], Mamori Kimizuka[10], Atsushi Suzuki[11], Kenji Shimizu[11], Hirofumi Ohashi[11], Nobuhiko Haga[12], Hironao Numabe[13], Emiko Horii[14], Toshiro Nagai[15], Hiroshi Yoshihashi[16], Gen Nishimura[17], Tatsushi Toda[18], Shuji Takada[19], Shigetoshi Yokoyama[19,22], Hiroshi Asahara[19,20], Shinichiro Sano[1,21], Maki Fukami[21], Shiro Ikegawa[2] and Tsutomu Ogata[1*]

Abstract

Background: Limb malformations are rare disorders with high genetic heterogeneity. Although multiple genes/loci have been identified in limb malformations, underlying genetic factors still remain to be determined in most patients.

Methods: This study consisted of 51 Japanese families with split-hand/foot malformation (SHFM), SHFM with long bone deficiency (SHFLD) usually affecting the tibia, or Gollop-Wolfgang complex (GWC) characterized by SHFM and femoral bifurcation. Genetic studies included genomewide array comparative genomic hybridization and exome sequencing, together with standard molecular analyses.

Results: We identified duplications/triplications of a 210,050 bp segment containing *BHLHA9* in 29 SHFM patients, 11 SHFLD patients, two GWC patients, and 22 clinically normal relatives from 27 of the 51 families examined, as well as in 2 of 1,000 Japanese controls. Families with SHFLD- and/or GWC-positive patients were more frequent in triplications than in duplications. The fusion point was identical in all the duplications/triplications and was associated with a 4 bp microhomology. There was no sequence homology around the two breakpoints, whereas rearrangement-associated motifs were abundant around one breakpoint. The rs3951819-*D17S1174* haplotype patterns were variable on the duplicated/triplicated segments. No discernible genetic alteration specific to patients was detected within or around *BHLHA9*, in the known causative SHFM genes, or in the exome.

(Continued on next page)

* Correspondence: tomogata@hama-med.ac.jp
†Equal contributors
[1]Department of Pediatrics, Hamamatsu University School of Medicine, Hamamatsu 431-3192, Japan
Full list of author information is available at the end of the article

(Continued from previous page)

Conclusions: These results indicate that *BHLHA9* overdosage constitutes the most frequent susceptibility factor, with a dosage effect, for a range of limb malformations at least in Japan. Notably, this is the first study revealing the underlying genetic factor for the development of GWC, and demonstrating the presence of triplications involving *BHLHA9*. It is inferred that a Japanese founder duplication was generated through a replication-based mechanism and underwent subsequent triplication and haplotype modification through recombination-based mechanisms, and that the duplications/triplications with various haplotypes were widely spread in Japan primarily via clinically normal carriers and identified via manifesting patients. Furthermore, genotype-phenotype analyses of patients reported in this study and the previous studies imply that clinical variability is ascribed to multiple factors including the size of duplications/triplications as a critical factor.

Keywords: *BHLHA9*, Split-hand/foot malformation, Long bone deficiency, Gollop-Wolfgang complex, Expressivity, Penetrance, Susceptibility, Japanese founder copy number gain

Introduction

Split-hand/foot malformation (SHFM), also known as ectrodactyly, is a rare limb malformation involving the central rays of the autopod [1,2]. It presents with median clefts of the hands and feet, aplasia/hypoplasia of the phalanges, metacarpals, and metatarsals, and syndactyly. SHFM results from failure to maintain the central portion of the apical ectodermal ridge (AER) in the developing autopod [1,2]. SHFM is divided into two forms: a non-syndromic form with limb-confined manifestations and a syndromic form with extra-limb manifestations [2]. Furthermore, non-syndromic SHFM can occur as an isolated abnormality confined to digits (hereafter, SHFM refers to this type) or in association with other limb abnormalities as observed in SHFM with long bone deficiency (SHFLD) usually affecting the tibia and in Gollop-Wolfgang complex (GWC) characterized by femoral bifurcation [1,2]. Both syndromic and non-syndromic forms are associated with wide expressivity and penetrance even among members of a single family and among limbs of a single patient [2].

SHFM and SHFLD are genetically heterogeneous conditions reviewed in ref. [2]. To date, SHFM has been identified in patients with heterozygous deletions or translocations involving the *DLX5–DLX6* locus at 7q21.2–21.3 (SHFM1) [3] (*DLX5* mutations have been detected recently), heterozygous duplications at 10q24 (SHFM3), heterozygous mutations of *TP63* at 3q27 (SHFM4), heterozygous deletions affecting *HOXD* cluster at 2q31 (SHFM5), and biallelic mutations of *WNT10B* at 12q31 (SHFM6); in addition, SHFM2 has been assigned to Xq26 by linkage analyses in a large Pakistani kindred [2]. Similarly, a genomewide linkage analysis in a large consanguineous family has identified two SHFLD susceptibility loci, one at 1q42.2–q43 (SHFLD1) and the other at 6q14.1 (SHFLD2); furthermore, after assignment of another SHFLD locus to 17p13.1–13.3 [4], duplications at 17p13.3 (SHFLD3) have been found in patients with SHFLD reviewed in ref. [2]. However, the GWC locus (loci) remains unknown at present.

The duplications at 17p13.3 identified to date are highly variable in size, and harbor *BHLHA9* as the sole gene within the smallest region of overlap [5-9]. *Bhlha9*/*bhlha9* is expressed in the limb bud mesenchyme underlying the AER in mouse and zebrafish embryos, and *bhlha9* knockdown has resulted in shortening of the pectoral fins in zebrafish [6]. Furthermore, *BHLHA9*-containing duplications have been identified not only in patients with SHFLD but also in those with SHFM and clinically normal family members [4-10]. These findings argue for a critical role of *BHLHA9* duplication in the development of SHFM and SHFLD, with variable expressivity and incomplete penetrance.

In this study, we report on *BHLHA9*-containing duplications/triplications with an identical fusion point and various haplotype patterns that were associated with a range of limb malformations including GWC, and discuss on characteristic clinical findings, genomic basis of Japanese founder copy number gains, and underlying factors for phenotypic variability.

Materials and methods

Patients/subjects

We studied 68 patients with SHFM (n = 55), SHFLD (n = 11), or GWC (n = 2), as well as 60 clinically normal relatives, from 51 Japanese families; the pedigrees of 27 of the 51 families and representative clinical findings are shown in Figure 1. All the probands 1–51 had a normal karyotype. Southern blot analysis for SHFM3 locus had been performed in 28 probands with SHFM, indicating 10q24 duplications in two of them [11]. Clinical features including photographs and roentgenograms of a proband with GWC and his brother with SHFLD (family 23 in Figure 1A) were as described previously [12]. The residencies of families 1–51 were widely distributed throughout Japan.

Ethical approval and samples

This study was approved by the Institutional Review Board Committees of Hamamatsu University School of

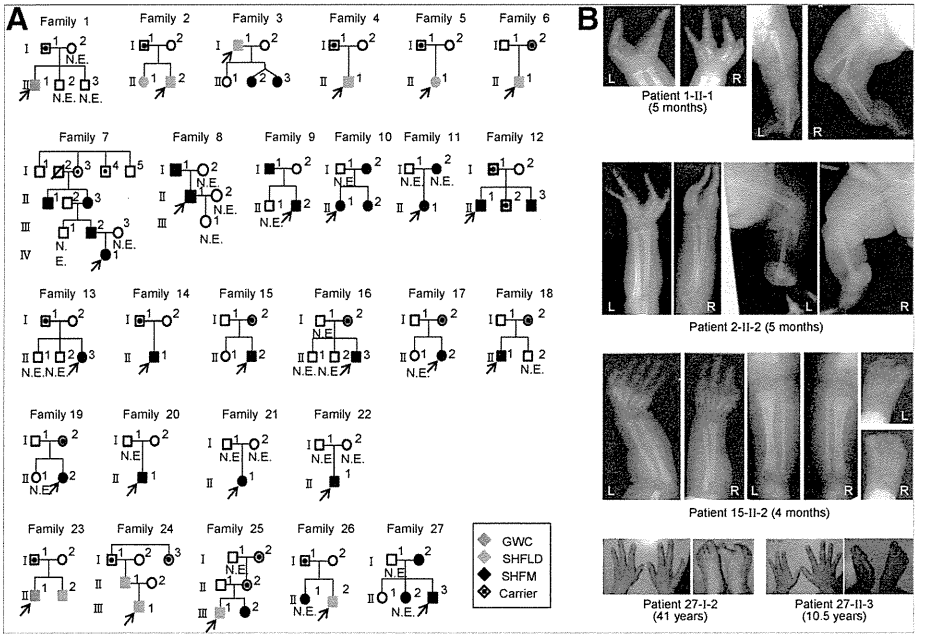

Figure 1 Clinical summary. A. Pedigrees of 27 Japanese families with duplications (families 1–22) and triplications (families 23–27) of a ~200 kb region involving *BHLHA9*. The duplications/triplications are associated with GWC, SHFLD, SHFM, or normal phenotype (carriers). N.E.: Not examined molecularly. **B**. Representative clinical findings. Each patient is indicated by a family-generation-individual style and corresponds to the patient/subject shown in Figure 1A and Additional file 5. The top panel: GWC with right bifid femur; the second panel: SHFLD with bilateral tibial deficiencies, the third panel: SHFM with polydactyly; and the bottom panel: SHFM.

Medicine, RIKEN, and National Center for Child Health and Development, and was performed using peripheral leukocyte samples after obtaining written informed consent for the molecular analysis and the publication of genetic and clinical data after removing information for personal identification (e.g., name, birthday, and facial photograph) from the adult subjects (^{3} 20 years) or from the parents of the child subjects (below 20 years). Furthermore, informed assent was also obtained from child subjects between 6–20 years.

Samples and primers

The primers utilized in this study are summarized in Additional file 1.

Molecular studies

Sanger sequencing, fluorescence *in situ* hybridization (FISH), microsatellite genotyping, Southern blotting, and bisulfite sequencing-based methylation analysis were performed by the standard methods, as reported previously [13]. Quantitative real-time PCR (qPCR) analysis was carried out by the SYBR Green methods on StepOnePlus system, using *RNaseP* as an internal control (Life Technologies). Genomewide oligonucleotide-based array comparative genomic hybridization (CGH) was performed with a catalog human array (4 × 180 K format, ID G4449A) according to the manufacturer's instructions (Agilent Technologies), and obtained copy number variants/polymorphisms were screened with Agilent Genomic Workbench software using the Database of Genomic Variants (http://dgv.tcag.ca/dgv/app/home). Sequencing of a long region encompassing *BHLHA9* was performed with the Nextera XT kit on MiSeq (Illumina), using SAMtools v0.1.17 software (http://samtools.sourceforge.net/). Exome sequencing was performed as described previously [14].

Assessment of genomic environments around the fusion points

Repeat elements around the fusion point were searched for using Repeatmasker (http://www.repeatmasker.org). Rearrangement-inducing DNA features were investigated for 300 bp regions at both the proximal and the distal sides of each breakpoint, using GEECEE (http://emboss.bioinformatics.nl/cgi-bin/emboss/geecee) for calculation of the average GC content, PALINDROME (http://mobyle.pasteur.fr/cgi-bin/portal.py#forms::palindrome) and Non-B DB (http://nonb.abcc.ncifcrf.gov) for the examination of the palindromes and non-B (non-canonical) structures, and Fuzznuc (http://emboss.bioinformatics.nl/cgi-bin/emboss/fuzznuc) for the assessment of rearrangement-associated sequence motifs and tri/tetranucleotides [15-20]. For controls, we examined 48 regions of 600 bp long selected at an interval of 1.5 Mb from the entire chromosome 17.

Statistical analysis

The statistical significance of the frequency was analyzed by the two-sided Fisher's exact probability test.

Results

Sequence analysis of the known causative/candidate genes

We performed direct sequencing for the previously known causative genes (*DLX5*, *TP63*, and *WNT10B*) reviewed in ref. [2] in the probands 1–51. Although no pathologic mutation was identified in *DLX5* and *TP63*, the previously reported homozygous missense mutation of *WNT10B* (c.944C > T, p.R332W) [21] was detected in the proband 48 with SHFM who was born to healthy consanguineous parents heterozygous for this mutation. In addition, while no variation was detected in *DLX5* and *WNT10B*, rs34201045 (4 bp insertion polymorphism) in *TP63* [21] was detected with an allele frequency of 61%.

We also examined *BHLHA9*, because gain-of-function mutations of *BHLHA9* as well as *BHLHA9*-harboring duplications may lead to limb malformations. No sequence variation was identified in the 51 probands.

Array CGH analysis

Array CGH analysis was performed for the probands 1–51, showing increased copy numbers at 17p13.3 encompassing *BHLHA9* (SHFLD3) in the probands 1–27 from families 1–27 (Figure 1A). Furthermore, heterozygous duplications at 10q24 (SHFM3) were detected in the probands 49–51, i.e., a hitherto unreported patient with paternally inherited SHFM (his father also had the duplication) and the two patients who had been indicated to have the duplications by Southern blot analysis [11]. No copy number alteration was observed at other SHFM/SHFLD loci in the probands 1–27 and 49–51. In the remaining probands 28–48, there was no copy number variation that was not registered in the Database of Genomic Variants.

Identical fusion points in *BHLHA9*-containing duplications/triplications

The array CGH indicated that the increased copy number regions at 17p13.3 were quite similar in the physical size in the probands 1–27 and present in three copies in the probands 1–22 and in four copies in the probands 23–27 (Figure 2A). Thus, FISH analysis was performed using 8,259 bp PCR products amplified from this region, showing two signals with a different intensity that was more obvious in the probands 23–27 (Figure 2A).

We next determined the fusion points of the duplications/triplications (Figure 2B). PCR products of 2,195 bp long were obtained with P1/P2 primers in the probands 1–27, and the fusion point was determined by direct sequencing for 418 bp PCR products obtained with P3/P4 primers. The fusion point was identical in all the probands 1–27; it resided on intron 1 of *ABR* and intron 1 of *YWHAE*, and was associated with a 4 bp microhomology.

Then, we performed qPCR analysis for a 214 bp region harboring the fusion point, using P5/P6 primers (Figure 2C and Additional file 2). The fusion point was present in a single copy in the probands 1–22 and in two copies in the probands 23–27. The results showed that the identical genomic segment harboring *BHLHA9* was tandemly duplicated in the probands 1–22 and triplicated in the probands 23–27. According to GRCh37/hg19 (http://genome.ucsc.edu/), the genomic segment was 210,050 bp long.

We also performed array CGH and qPCR for the fusion point in 15 patients other than the probands and 47 clinically normal relatives from the 27 families (Figures 1 and 2C). The duplications/triplications were identified in all the 15 patients. Thus, in a total of 42 patients, duplications/triplications were found in 29 SHFM patients, 11 SHFLD patients, and two GWC patients. Furthermore, the duplications/triplications were also present in 22 of the 47 clinically normal relatives. In particular, they were invariably identified in either of the clinically normal parents when both of them were examined; they were also present in other clinically normal relatives in families 7, 12, 24, and 25.

Since the above data indicated the presence of duplications/triplications in clinically normal subjects, we performed qPCR for the fusion point in 1,000 Japanese controls. The fusion point was detected in a single copy in two subjects (Subjects 1 and 2 in Figure 2C). We also performed array CGH in 200 of the 1,000 controls including the two subjects, confirming the duplications in the two subjects and lack of other copy number variations, including deletions involving *BHLHA9*, which were not registered in the Database of Genomic Variants in the 200 control subjects. The frequency of duplications/triplications was significantly higher in the probands than in the control subjects (27/51 vs. 2/1,000, $P = 3.5 \times 10^{-37}$).

Various haplotype patterns on the duplicated/triplicated segments

We carried out genotyping for rs3951819 (A/G SNP on *BHLHA9*) and *D17S1174* (CA repeat microsatellite locus) on the genomic segment subjected to duplications/triplications (Figure 2A), and determined rs3951819-*D17S1174* haplotype patterns. Representative results are shown in Figure 2D, and all the data are available on request. Various haplotype patterns were identified on the single, the duplicated, and the triplicated segments, and the [A-14] haplotype was most prevalent on the duplicated/triplicated segments (Table 1). While the distribution of CA repeat lengths on the single segments was discontinuous, similar discontinuous distribution was

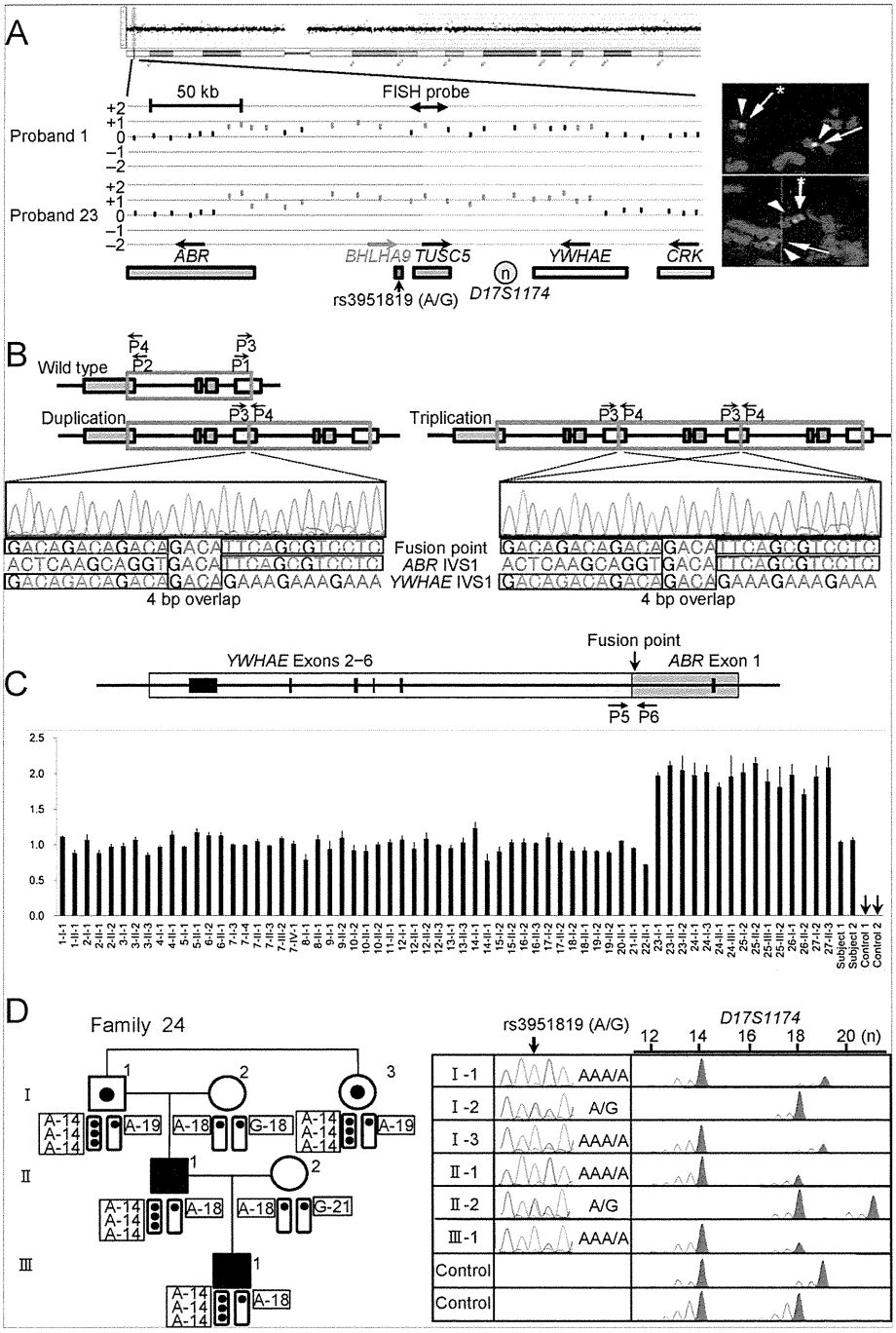

Figure 2 (See legend on next page.)

(See figure on previous page.)
Figure 2 Identification and characterization of the duplications/triplications involving *BHLHA9* at chromosome 17p13.3. A. Array CGH and FISH analyses in proband 1 and proband 23 with GWC. In array CGH analysis, the black and the red dots denote the normal and the increased copy numbers, respectively. Since the log2 signal ratios for a ~200 kb region encompassing *BHLHA9* are around +0.5 in the proband 1 and around +1.0 in the proband 23, this indicates the presence of three and four copies of this region in the two probands, respectively. In FISH analysis, two red signals with an apparently different density are detected by the 8,289 bp PCR probe (the stronger signals are indicated with asterisks). The green signals derive from an internal control probe (CEP17). The arrows on the genes show transcriptional directions. Rs3951819 (A/G) resides within *BHLHA9*. **B**. Determination of the fusion point. The fusion has occurred between intron 1 of *ABR* and intron 1 of *YWHAE*, and is associated with a 4 bp (GACA) microhomology. P1–P4 show the position of primers. **C**. Quantitative real-time PCR analysis. The upper part denotes the fusion point. P5 & P6 show the position of primers. The lower part shows the copy number of the fusion point in patients/subjects with duplications/triplications (indicated by a family-generation-individual style corresponding to that in Figure 1 and Additional file 5). Subject-1 and subject-2 denote the two control subjects with the duplication, and control-1 and control-2 represent normal subjects without the duplication/triplication. **D**. The rs3951819 (A/G SNP)–*D17S1174* (CA repeat number) haplotype patterns in family 24. Assuming no recombination between rs3951819 and *D17S1174*, the haplotype patterns of the family members are determined as shown here. The haplotype patterns of the remaining families have been interpreted similarly.

also observed in the Japanese general population (see Additional file 3).

Genomic environments around the breakpoints

The breakpoint on *YWHAE* intron 1 resided on a simple *Alu* repeat sequence, and that on *ABR* intron 1 was present on a non-repetitive sequence. There was no low copy repeat around the breakpoints. Comparison of the frequencies of known rearrangement-inducing DNA features between 600 bp sequences around the breakpoints and those of 48 regions selected at an interval of 1.5 Mb from chromosome 17 revealed that palindromes, several types of non-B DNA structures, and a rearrangement-associated sequence motif were abundant around the breakpoint on *YWHAE* intron 1 (see Additional file 4).

Clinical findings of families 1–27

Clinical assessment revealed several notable findings. First, duplications/triplications were associated with SHFM, SHFLD, GWC, or normal phenotype, with inter- and intra-familial clinical variability (Figure 1A). Second, in the 42 patients, split hand (SH) was more prevalent than split foot (SF) (41/42 vs. 17/42, $P = 6.2 \times 10^{-9}$), and long bone defect (LBD) was confined to lower extremities (0/42 vs. 13/42, $P = 4.1 \times 10^{-5}$) (Table 2 and Additional file 5). Third, there was no significant sex difference in the ratio between patients with limb malformations and patients/carriers with duplications/triplications (26/38 in males vs. 16/26 in females, $P = 0.60$) (Table 2 and Additional file 5). Fourth, the ratio of LBD positive families was significantly higher in triplications than in duplications (4/5 vs. 16/22, $P = 0.047$) (Figure 1A and Table 2). Fifth, while the duplications/triplications were transmitted from patients to patients, from carriers to patients, and from a carrier to a carrier (from I-1 to II-2 in family 12), transmission from a patient to a carrier was not identified (Figure 1A); it should be pointed out, however, that molecular analysis in a clinically normal child born to an affected parent was possible only in a single adult subject (II-1 in family 27), and that molecular analysis in clinically

Table 1 The rs3951819 (A/G SNP) – *D17S1174* (CA repeat number) haplotype

Patterns of the 210,050 bp segment subjected to copy number gains	
Haplotype pattern	**Family**
<Single segment>	
[A-14]	1, 5, 9, 15, 17, 19, 23, 26
[A-16]	12
[A-18]	3, 14, 15, 24, 25, 26
[A-19]	2, 6, 13, 19, 20, 24, 25, 27
[A-21]	5, 23
[G-12]	17
[G-14]	2, 3, 6, 12, 13, 19, 26
[G-18]	3, 5, 17, 18, 24, 25
[G-19]	9, 12, 18, 20, 25
[G-21]	1, 9, 19, 24, 27
[A-14] or [G-14]	16
[A-18] or [G-18]	4
[A-19] or [G-19]	4
[A-21] or [G-21]	16
<Duplicated segments>	
[A-14] + [A-14]	5, 12, 13, 14, 15, 20
[A-14] + [A-18]	1
[A-14] + [G-18] or [G-14] + [A-18]	2, 3, 4, 6, 9, 16, 17
[A-14] + [G-18] or [A-14] + [G-19]	18
[A-14] + [G-14] or [G-14] + [G-14]	19
<Triplicated segments>	
[A-14] + [A-14] + [A-14]	23, 24
[A-14] + [A-14] + [G-14]	25
[A-14] + [A-19] + [A-19]	26
[A-14] + [G-18] + [G-18] or [G-14] + [A-18] + [G-18]	27

The haplotype patterns written in the left column have been detected in at least one patient/subject in the families described in the right column.
Genotyping could not be performed in several patients/subjects who had been repeatedly examined previously, because of the extremely small amount of DNA samples that were virtually used up in the sequencing and array CGH analyses.

Table 2 Summary of clinical findings in patients/carriers with duplications/triplications involving *BHLHA9*

	SHFM (+) patients			LBD (+) patients			Patient ratio*			LBD (+) families		
	SH	SF	*P*-value	U-LBD	L-LBD	*P*-value	Male	Female	*P*-value	Trip	Dup	*P*-value
This study	41/42	17/42	6.2×10^{-9}	0/42	13/42	4.1×10^{-5}	26/38	16/26	0.60	4/5	16/22	0.047
Previous studies	63/84	23/84	8.6×10^{-10}	11/91	42/91	5.7×10^{-7}	68/114	31/79	5.7×10^{-3}	...	...	...
Sum	104/126	40/126	1.1×10^{-16}	11/133	55/133	3.0×10^{-10}	94/152	47/105	7.6×10^{-3}	...	...	...

SHFM: split-hand/foot malformation; SH: split hand; SF: split foot; LBD: long bone deficiency; U: upper; L: lower; Trip: triplication; and Dup: duplication.
In the previous studies, patients without detailed phenotypic description and those of unknown sex have been excluded (3–9).
*The ratio between patients with limb malformations and patients/carriers with duplications/triplications, i.e. the number of patients over the number of patients plus carriers.

normal children <20 years old was possible only in two subjects (II-2 in family 12 and II-1 in family 15). Lastly, limb malformation was inherited in an apparently autosomal dominant manner (from patients to patients), or took place as an apparently *de novo* event or as an apparently autosomal recessive trait (from clinically normal parents to a single or two affected children) (Figure 1A).

Attempts to identify a possible modifier(s)

The variable expressivity and incomplete penetrance in families 1–27 suggest the presence of a possible modifier (s) for the development of limb malformations. Thus, we performed further molecular studies in patients/subjects in whom DNA samples were still available, and compared the molecular data between patients with SHFM and those with SHFLD for the assessment of variable expressivity and between SHFM, SHFLD, or total patients and carriers for the evaluation of incomplete penetrance.

We first examined the possibility that the modifier(s) resides within or around *BHLHA9* (see Additional file 6). There was no *BHLHA9* mutation in all the 21 examined probands with SHFM, SHFLD, or GWC, as described in the section of "Sequence analysis of the known causative/candidate genes". The rs3951819 A/G SNP pattern on the duplicated/triplicated segments was apparently identical between patients and carriers (e.g. Figure 2D), and the frequency of A/G allele on the normal chromosome 17 was similar between SHFM and SHFLD patients and between SHFM, SHFLD, or total patients and carriers (see Additional file 7). The results of other known SNPs on *BHLHA9* (rs185242872, rs18936498, and rs140504068) were not informative, because of absence or extreme rarity of minor alleles. Furthermore, in SHFM families 7, 12, and 18, sequencing of a 7,406 bp region encompassing *BHLHA9* and Southern blot analysis using five probes and *Mfe*I-, *Ssp*I-, and *Sac*I-digested genomic DNA revealed no variation specific to the patients, and methylation analysis for a CpG rich region at the upstream of *BHLHA9* delineated massive hypomethylation in all the patients/carriers examined.

Next, we examined the possibility that a variant(s) of known causative genes constitutes the modifier(s). Since rs34201045 in *TP63* was identified in the mutation analysis, we compared rs34201045 genotyping data between the 27 probands and the 15 carriers. The allele and genotype frequencies were similar between SHFM and SHFLD patients and between SHFM, SHFLD, or total patients and carriers (see Additional file 8).

We finally performed exome sequencing in SHFM families 13 and 17–19. However, there was no variation specific to the patients. In addition, re-examination of the genomewide array CGH data showed no discernible copy number variation specific to the patients.

Discussion

BHLHA9 overdosage and clinical characteristics

We identified duplications/triplications of a ~ 200 kb genomic segment involving *BHLHA9* at 17p13.3 in 27 of 51 families with SHFM, SHFLD, or GWC. To our knowledge, this is the first study revealing the underlying genetic factor for the development of GWC, and demonstrating the presence of triplications involving *BHLHA9* that were suggested but not confirmed in the previous studies [5,9]. Furthermore, this study indicates that *BHLHA9*-containing duplications/triplications are the most frequent underlying factor for the development of limb malformations at least in Japan. Notably, SHFLD and GWC with LBD were significantly more frequent in patients with triplications than in those with duplications, and the duplications/triplications were identified in clinically normal familial members and in the general population. These findings imply that increased *BHLHA9* copy number constitutes a strong susceptibility, rather than a causative, factor with a dosage effect for the development of a range of limb malformations. Since *Bhlha9* is expressed in the developing ectoderm adjacent to the AER rather than the AER itself in mouse embryos [6], *BHLHA9* appears to play a critical role in the limb development by interacting with the AER. While the duplications/triplications identified in this study included *TUSC5* and generated an *ABR-YWHAE* chimeric gene (Figure 2C), *TUSC5* duplication and the chimeric gene formation are not common findings in the previously reported patients with duplications at 17p13.3 and SHFM and/or SHFLD [5-9]. In addition, none of *Tusc5*, *Abr*, and *Ywhae* is specifically expressed in the developing mouse limb buds [22] (A Transcriptome Atlas Database

for Mouse Embryo of Eurexpress Project, http://www.eurexpress.org/ee/project/).

Several clinical findings are noteworthy in patients/subjects with duplications/triplications. First, SH was more frequent than SF in this study as well as in the previous studies, and LBD was confined to lower extremities in this study and was more frequent in lower extremities than in upper extremities in the previous studies (Table 2) [4-10]. This implies that *BHLHA9* overdosage exerts differential effects on the different parts of limbs. Second, while limb malformations were similarly identified between males and females in this study, they were more frequently observed in males than in females in the previous studies (Table 2) [4-10]. In this regard, it has been reported that testosterone influences the digital growth pattern as indicated by the lower second to fourth digit length ratio in males than in females [23-25], and that Caucasian males have higher serum testosterone values and lower second to fourth digit length ratios than Oriental males [26,27]. Such testosterone effects on the digital growth pattern with ethnic difference may explain why male dominant manifestation was observed in the previous studies primarily from Caucasian countries and was not found in this study. Lastly, LBD was more prevalent in patients with triplications than in those with duplications. This suggests that LBD primarily occurs when the effects of *BHLHA9* overdosage are considerably elevated.

Genomic basis of the Japanese founder copy number gains

The duplications/triplications were associated with the same fusion point and variable haplotype patterns. Since there was no sequence homology or low-copy repeats around the breakpoints, it is unlikely that such duplications/triplications were recurrently produced in different individuals by non-allelic homologous recombination (NAHR) [17,20]. Instead, it is assumed that a Japanese founder duplication took place in a single ancestor, and was spread with subsequent triplication and modification of the haplotype patterns.

The most likely genomic basis of the Japanese duplications/triplications is illustrated in Additional file 9. Notably, a 4 bp (GACA) microhomology was identified at the duplication fusion point (Figure 2B). A microhomology refers to two to five nucleotides common to the sequences of the two breakpoints, and is found as an overlapping sequence at the join point [16,19,20]. This suggests that the Japanese founder duplication was generated by replication-based mechanisms such as fork stalling and template switching (FoSTeS) and microhomology-mediated break-induced replication (MMBIR), because the presence of such a microhomology is characteristic of FoSTeS/MMBIR [17-20]. Indeed, such a simple tandem duplication with a microhomology can be produced by one time FoSTeS/MMBIR [17-20], although it could also be generated by non-homologous end-joining (NHEJ) [17]. Since the [A-14] haplotype was most prevalent on the duplicated/triplicated segments, it is inferred that a genomic rearrangement occurred in an ancestor with the [A-14] haplotype, yielding the founder duplication with the [A-14] + [A-14] haplotype. Furthermore, the presence of multiple stimulants for genomic rearrangements around the breakpoint on *YWHAE* intron 1 would have facilitated the generation of the founder duplication. In particular, non-B structures are known to stimulate the occurrence of both replication-based FoSTeS/MMBIR and double-strand breaks and resultant NHEJ [17,28,29], although the relative importance of each non-B DNA structure is largely unknown.

Subsequent triplication and haplotype modification can develop from the Japanese founder duplication through unequal interchromatid and interchromosomal recombinations [17,20]. Indeed, a tandem triplication with the [A-14] + [A-14] + [A-14] haplotype can be generated by unequal exchange between sister chromatids with the [A-14] + [A-14] haplotype, and various haplotype patterns are yielded by unequal interchromosomal exchanges involving the duplicated or triplicated segments. Furthermore, the haplotype variation would be facilitated by unequal exchanges between sister chromatids harboring duplications/triplications with various haplotype patterns and by the further unequal interchromosomal exchanges.

Underlying factors for the phenotypic variability

The duplications/triplications were accompanied by limb malformations with variable expressivity and incomplete penetrance. Although this may suggest the presence of a possible modifier(s) for the development of limb malformations, such a modifier(s) was not detected. In particular, while patient-to-carrier transmission of duplications/triplications was not identified in this study, even patient-to-carrier-to-patient transmission has been reported in three pedigrees [5,6,10]. Such transmission pattern with incomplete penetrance characterized by skipping of a generation is apparently inexplicable by assuming a modifier (s) interacting with *BHLHA9* or independent of *BHLHA9* on the duplication/triplication positive chromosome 17, on the normal chromosome 17, or on other chromosomes (Figure 3, Models A, B, and C, see also the legends in Figure 3).

In this regard, it is noteworthy that the development of limb malformations is obviously dependent on the size of genomic segment subjected to copy number gains. Actually, limb malformation has occurred in only one of 21 large duplications encompassing *BHLHA9* (average 1.55 Mb, mean 1.12 Mb) and in 29 of 80 small duplications encompassing *BHLHA9* (average 244 kb, mean 263 kb) ($P = 5.9 \times 10^{-3}$) [8]. Consistent with this, the patients with large and

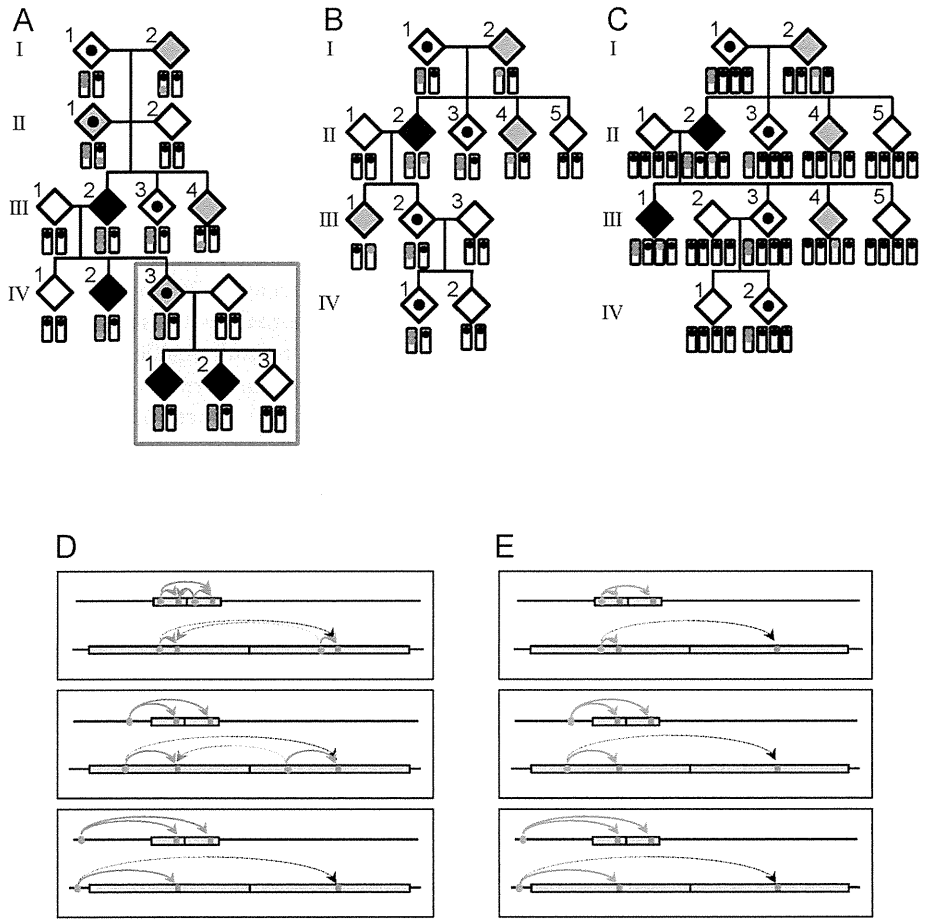

Figure 3 Models for a modifier(s) and effects of the duplication size. In models **A–C**, the yellow bars show chromosome 17, and the light green bars indicate other chromosomes. The two red dots represent the duplication at 17p13.3, and the blue dots indicate a putative modifier(s). Black painted diamonds represent limb malformation positive patients, dot-associated and gray painted diamonds indicate clinically normal carriers with the duplications and the modifier(s) respectively, and white painted diamonds denote clinically normal subjects without both the duplications and the modifier(s). **A**. This model assumes that co-existence of the duplication and a *cis*-acting modifier(s) causes limb malformation. If co-existence of the duplication and the *cis*-acting modifier(s) is associated with incomplete penetrance, this can explain all the transmission patterns observed to date, including the patient-to-carrier transmission and the presence of ≥ 2 affected children. **B**. This model postulates that the presence of a *cis*-acting modifier(s) on the normal chromosome 17 leads to limb malformation by enhancing the expression of the single *BHLHA9*, together with duplicated *BHLHA9* on the homologous chromosome. **C**. This model postulates that co-existence of the duplication at 17p13.3 and a modifier(s) on other chromosome causes limb malformation. In models **D–E**, the red bars represent *BHLHA9*, the blue circles indicate a physiological cis-regulatory element for *BHLHA9*, and the green circles indicate a non-physiological modifier(s) for *BHLHA9*. **D**. The physiological cis-regulatory element may be duplicated or non-duplicated, depending on its position relative to the size of the duplications. *BHLHA9* expression can be higher in small duplications than large duplications. **E**. The non-physiological modifier(s) can be transferred to various positions of the duplication positive chromosome 17, depending on the recombination places (see Model A). *BHLHA9* expression can be higher in small duplications than large duplications irrespective of the position of the modifier(s).

small duplications were ascertained primarily due to developmental retardation and limb malformation, respectively [8]. It is likely that a physiological cis-regulatory element for *BHLHA9* (e.g., an enhancer) can frequently but not invariably work on both of the duplicated *BHLHA9* when the duplication size is small but is usually incapable of working on duplicated *BHLHA9* when the duplication size is large, probably because of the difference in the chromatin structure (see Model D in Figure 3). Similar findings have also been reported in other genes. For example, small (~150 kb) and relatively small (600–800 kb) duplications involving a putative testis-specific enhancer(s) for *SOX9* have caused 46,XX testicular and ovotesticular disorders of sex development respectively, whereas large duplications (~2 Mb) involving the enhancer(s) have permitted normal ovarian development in 46,XX individuals [30].

Thus, a plausible explanation may be that a range of limb malformations emerge when the effects of *BHLHA9* overdosage exceed the threshold for the development of SHFM, SHFLD, or GWC, depending on the conditions of

other genetic and environmental factors including the size of duplications/triplications as an important but not definitive factor. One may argue that this notion is inconsistent with the apparent anticipation phenomenon that is suggested by the rare patient-to-carrier transmission and the frequent carrier-to-patient transmission of the duplications/triplications, because no specific factor(s) exaggerating the development of limb malformations is postulated in the next generation. However, the skewed transmission pattern would primarily be ascribed to ascertainment bias rather than anticipation [31]. Indeed, while clinically normal parents of disease positive children would frequently be examined for the underlying genetic factor(s) of the children, clinically normal children born to disease positive parents would not usually be studied for such factor(s), as exemplified in this study. Similarly, the frequent patient-to-patient transmission of the duplications/triplications would also be ascribed to ascertainment bias, because molecular studies would preferentially be performed in such families. Nevertheless, the apparently autosomal dominant inheritance pattern of limb malformations in several families may still suggest the relevance of a non-physiological *cis*-acting modifier(s) (see Models A and E in Figure 3). It is possible that such a modifier(s), once transferred onto the duplication/triplication positive chromosome 17, is usually co-transmitted with the duplications/triplications, leading to a specific condition in which the effects of *BHLHA9* overdosage frequently but not invariably exceed the threshold for the development of limb malformations in offsprings with the duplications/triplications.

Remarks

Several matters should be pointed out in the present study. First, in contrast to diverse duplication sizes in non-Japanese populations [5-9], the size of the genomic segment subjected to duplications/triplications was identical in this study. Since families 1–27 were derived from various places of Japan, there is no selection bias in terms of a geographic distribution. Rather, since the small duplications/triplications identified in this study were not associated with developmental retardation, it is likely that they spread throughout Japan primarily via carriers with normal fitness and were found via patients with limb malformations. Obviously, this notion does not exclude the possible presence of other types of duplications/triplications at 17p13.3 in Japan. Second, except for the duplications/triplications at 17p13.3, we could reveal a homozygous *WNT10B* mutation (SHFM6) only in a single SHFM family and chromosome 10q24 duplications (SHFM3) only in three SHFM families. Thus, underlying factors are still unknown in the remaining 20 families, although tiny deletions and/or duplications affecting the known SHFM loci might have been overlooked because of the low resolution of the array. In addition, although all the probands had a normal karyotype, there might be cryptic translocations and/or inversions involving the known SHFM loci. Third, no deletion of *BHLHA9* was identified in the 51 probands and in the 200 control subjects. This argues against the relevance of *BHLHA9* haploinsufficiency to limb malformations, and coincides with the Japanese founder duplication being produced by a replication-mediated mechanism rather than an interchromatid/interchromosomal (but not an intrachromatid) NAHR that can lead to both deletions and duplications as a mirror image [17]. Furthermore, it remains to be determined (i) whether gain-of-function mutations (and possibly loss-of-function mutations as well) of *BHLHA9* are identified in patients with limb malformations, (ii) whether duplications/triplications involving *BHLHA9* underlie limb malformations other than SHFM, SHFLD, and GWC, and (iii) whether *BHLHA9*-containing duplications/triplications are also the most frequent underlying factors for limb malformations in non-Japanese populations.

Conclusions

The results imply that (i) duplications/triplications involving *BHLHA9* at chromosome 17p13.3 constitute a strong susceptibility factor for the development of a range of limb malformations including SHFM, SHFLD, and GWC; (ii) the Japanese founder duplication was generated by a replication-based mechanism and spread with subsequent triplication and haplotype modification through recombination-based mechanisms; and (iii) clinical variability appears to be due to multiple factors including the size of duplications/triplications. Thus, the present study provides useful information on the development of limb malformations.

Additional files

Additional file 1: Table S1. Primers utilized in this study.

Additional file 2: Figure S1. Real-time PCR analysis.

Additional file 3: Figure S2. *D17S1174* analysis in 200 Japanese control subjects, showing discontinuous distribution of the CA repeat numbers, as observed in the Japanese families with limb malformations.

Additional file 4: Table S2. *In silico* analysis for specific structures around the breakpoint-flanking regions and control regions.

Additional file 5: Table S3. Phenotypes in patients/subjects with increased copy number of *BHLHA9*.

Additional file 6: Figure S3. Genomic region encompassing *BHLHA9* examined in this study.

Additional file 7: Table S4. Polymorphism analysis of rs3951819 (A/G SNP) in *BHLHA9*.

Additional file 8: Table S5. Polymorphism analysis of rs34201045 (4 bp insertion) in *TP63*.

Additional file 9: Figure S4. Genomic basis of the Japanese founder copy number gain.

Abbreviations

AER: Apical ectodermal ridge; CEP17: Centromere of chromosome 17; CGH: Comparative genomic hybridization; Dup: Duplication; FoSTeS: Fork stalling and template switching; GWC: Gollop-Wolfgang complex; L: Lower; LBD: Long bone defect; MMBIR: Microhomology-mediated break-induced replication; NAHR: Non-allelic homologous recombination; N.E.: Not examined; NHEJ: Non-homologous end-joining; qPCR: Quantitative real-time PCR; SF: Split foo17)t; SH: Split hand; SHFLD: SHFM with long bone deficiency; SHFM: Split-hand/foot malformation; Trip: Triplication; U: Upper.

Competing interests

The authors have nothing to declare.

Authors' contributions

Molecular analysis using human samples was performed by EN, HK, FK. RY, SN, SW, KY, TT, SS, MF, and TT, ST, and SY; clinical assessment and blood sampling by RK, HT, SM, TK, TH, MK, AS, KS, HO, NH, HN, EH, TN, HY, GN, and TO; design of this study and interpretations of the data by HA, SI, and TO; and paper writing by TO. All authors read and approved the final manuscript.

Acknowledgements

This work was supported in part by Grants-in-Aid for Scientific Research on Innovative Areas [22132004-A01] from the Ministry of Education, Culture, Sports, Science and Technology, by Grant for Research on Intractable Diseases from the Ministry of Health, Labor and Welfare [H24-048], and by Grants from National Center for Child Health and Development [23A-1, 24–7]. The funders had no role in study design, data collection and analysis, decision to publish, or preparation of the manuscript.

Author details

[1]*Department of Pediatrics, Hamamatsu University School of Medicine,* Hamamatsu 431-3192, Japan. [2]Laboratory of Bone and Joint Diseases, Center for Integrative Medical Sciences, RIKEN, Tokyo, Japan. [3]Department of Orthopedic Surgery, Tokyo, Japan. [4]Division of Medical Genetics, National *Center for Child Health and Development, Tokyo,* Japan. [5]*Section of Clinical* Genetics, Department of Pediatrics, Tenshi Hospital, Sapporo, Japan. [6]Department of Pediatrics, Central Hospital, Aichi Human Service Center, Kasugai, Japan. [7]Department of Human Genetics, Nagasaki University Graduate School of Biomedical Sciences, Nagasaki, Japan. [8]Department of Medical Genetics, Shinshu University School of Medicine, Matsumoto, Japan. [9]Department of Pediatrics, Keio University School of Medicine, Tokyo, Japan. [10]Department of Orthopedics, National Rehabilitation Center for Disabled Children, Tokyo, Japan. [11]Division of Medical Genetics, Saitama Children's Medical Center, Saitama, Japan. [12]Department of Rehabilitation Medicine, University of Tokyo, Tokyo, Japan. [13]Department of Genetic Counseling, Graduate School of Humanities and Sciences, Ochanomizu University, Tokyo, Japan. [14]Department of Orthopedic Surgery, Japanese Red Cross Nagoya Daiichi Hospital, Nagoya, Japan. [15]Department of Pediatrics, Dokkyo Medical University Koshigaya Hospital, Koshigaya, Japan. [16]Division of Medical Genetics, Tokyo, Japan. [17]Department of Pediatric Imaging, Tokyo Metropolitan Children's Medical Center, Tokyo, Japan. [18]Division of Neurology/Molecular Brain Science, Kobe University Graduate School of Medicine, Kobe, Japan. [19]Department of Systems Biomedicine, National Research Institute for Child Health and Development, Tokyo, Japan. [20]Department of Systems Biomedicine, Graduate School of Medical and Dental Sciences, Tokyo Medical and Dental University, Tokyo, Japan. [21]Department of Molecular Endocrinology, National Research Institute for Child Health and Development, Tokyo, Japan. [22]Present address: Laboratory of Metabolism Center for Cancer Research, National Cancer Institute, Bethesda, MD, USA.

Received: 15 April 2014 Accepted: 22 July 2014
Published online: 21 October 2014

References

1. Duijf PH, van Bokhoven H, Brunner HG: **Pathogenesis of split-hand/split-foot malformation.** *Hum Mol Genet* 2003, **12**:R51–60.
2. Gurrieri F, Everman DB: **Clinical, genetic, and molecular aspects of split-hand/foot malformation: an update.** *Am J Med Genet A* 2013, **161A**:2860–2672.
3. Lango Allen H, Caswell R, Xie W, Xu X, Wragg C, Turnpenny PD, Turner CL, Weedon MN, Ellard S: **Next generation sequencing of chromosomal rearrangements in patients with split-hand/split-foot malformation provides evidence for DYNC1/1 exonic enhancers of DLX5/6 expression in humans.** *J Med Genet* 2014, **51**:264–267.
4. Lezirovitz K, Maestrelli SR, Cotrim NH, Otto PA, Pearson PL, Mingroni-Netto RC: **A novel locus for split-hand/foot malformation associated with tibial hemimelia (SHFLD syndrome) maps to chromosome region 17p13.1-17p13.3.** *Hum Genet* 2008, **123**:625–631.
5. Armour CM, Bulman DE, Jarinova O, Rogers RC, Clarkson KB, DuPont BR, Dwivedi A, Bartel FO, McDonell L, Schwartz CE, Boycott KM, Everman DB, Graham GE: **17p13.3 microduplications are associated with split-hand/foot malformation and long-bone deficiency (SHFLD).** *Eur J Hum Genet* 2011, **19**:1144–1151.
6. Klopocki E, Lohan S, Doelken SC, Stricker S, Ockeloen CW, Soares Thiele de Aguiar R, Lezirovitz K, Mingroni Netto RC, Jamsheer A, Shah H, Kurth I, Habenicht R, Warman M, Devriendt K, Kordass U, Hempel M, Rajab A, Mäkitie O, Naveed M, Radhakrishna U, Antonarakis SE, Horn D, Mundlos S: **Duplications of BHLHA9 are associated with ectrodactyly and tibia hemimelia inherited in non-Mendelian fashion.** *J Med Genet* 2012, **49**:119–125.
7. Petit F, Andrieux J, Demeer B, Collet LM, Copin H, Boudry-Labis E, Escande F, Manouvrier-Hanu S, Mathieu-Dramard M: **Split-hand/foot malformation with long-bone deficiency and BHLHA9 duplication: two cases and expansion of the phenotype to radial agenesis.** *Eur J Med Genet* 2013, **56**:88–92.
8. Curry CJ, Rosenfeld JA, Grant E, Gripp KW, Anderson C, Aylsworth AS, Saad TB, Chizhikov VV, Dybose G, Fagerberg C, Falco M, Fels C, Fichera M, Graakjaer J, Greco D, Hair J, Hopkins E, Huggins M, Ladda R, Li C, Moeschler J, Nowaczyk MJ, Ozmore JR, Reitano S, Romano C, Roos L, Schnur RE, Sell S, Suwannarat P, Svaneby D, *et al*: **The duplication 17p13.3 phenotype: analysis of 21 families delineates developmental, behavioral and brain abnormalities, and rare variant phenotypes.** *Am J Med Genet A* 2013, **161A**:1833–1852.
9. Luk HM, Wong VC, Lo IF, Chan KY, Lau ET, Kan AS, Tang MH, Tang WF, She WM, Chu YW, Sin WK, Chung BH: **A prenatal case of split-hand malformation associated with 17p13.3 triplication - a dilemma in genetic counseling.** *Eur J Med Genet* 2014, **57**:81–84.
10. Petit F, Jourdain AS, Andrieux J, Baujat G, Baumann C, Beneteau C, David A, Faivre L, Gaillard D, Gilbert-Dussardier B, Jouk PS, Le Caignec C, Loget P, Pasquier L, Porchet N, Holder-Espinasse M, Manouvrier-Hanu S, Escande F: **Split hand/foot malformation with long-bone deficiency and BHLHA9 duplication: report of 13 new families.** *Clin Genet* 2014, **85**:464–469.
11. Kano H, Kurosawa K, Horii E, Ikegawa S, Yoshikawa H, Kurahashi H, Toda T: **Genomic rearrangement at 10q24 in non-syndromic split-hand/split-foot malformation.** *Hum Genet* 2005, **118**:477–483.
12. Matsuyama J, Mabuchi A, Zhang J, Iida A, Ikeda T, Kimizuka M, Ikegawa S: **A pair of sibs with tibial hemimelia born to phenotypically normal parents.** *J Hum Genet* 2003, **48**:173–176.
13. Kagami M, Sekita Y, Nishimura G, Irie M, Kato F, Okada M, Yamamori S, Kishimoto H, Nakayama M, Tanaka Y, Matsuoka K, Takahashi T, Noguchi M, Tanaka Y, Masumoto K, Utsunomiya T, Kouzan H, Komatsu Y, Ohashi H, Kurosawa K, Kosaki K, Ferguson-Smith AC, Ishino F, Ogata T: **Deletions and epimutations affecting the human 14q32.2 imprinted region in individuals with paternal and maternal upd(14)-like phenotypes.** *Nat Genet* 2008, **40**:237–242.
14. Iida A, Okamoto N, Miyake N, Nishimura G, Minami S, Sugimoto T, Nakashima M, Tsurusaki Y, Saitsu H, Shiina M, Ogata K, Watanabe S, Ohashi H, Matsumoto N, Ikegawa S: **Exome sequencing identifies a novel INPPL1 mutation in opsismodysplasia.** *J Hum Genet* 2013, **58**:391–394.
15. Cer RZ, Donohue DE, Mudunuri US, Temiz NA, Loss MA, Starner NJ, Halusa GN, Volfovsky N, Yi M, Luke BT, Bacolla A, Collins JR, Stephens RM: **Non-B DB v2.0: a database of predicted non-B DNA-forming motifs and its associated tools.** *Nucl Acids Res* 2013, **41**:D94–D100.
16. Kornreich R, Bishop DF, Desnick RJ: **α-Galactosidase A gene rearrangements causing Fabry disease: identification of short direct repeats at breakpoints in an Alu-rich gene.** *J Biol Chem* 1990, **265**:9319–9326.
17. Gu W, Zhang F, Lupski JR: **(2008) Mechanisms for human genomic rearrangements.** *Pathogenetics* 2008, **1**:4.
18. Vissers LE, Bhatt SS, Janssen IM, Xia Z, Lalani SR, Pfundt R, Derwinska K, de Vries BB, Gilissen C, Hoischen A, Nesteruk M, Wisniowiecka-Kowalnik B, Smyk

M, Brunner HG, Cheung SW, van Kessel AG, Veltman JA, Stankiewicz P: **Rare pathogenic microdeletions and tandem duplications are microhomology-mediated and stimulated by local genomic architecture.** *Hum Mol Genet* 2009, **18**:3579–3593.
19. Hastings PJ, Ira G, Lupski JR: **A microhomology-mediated break-induced replication model for the origin of human copy number variation.** *PLoS Genet* 2009, **5**:e1000327.
20. Colnaghi R, Carpenter G, Volker M, O'Driscoll M: **The consequences of structural genomic alterations in humans: genomic disorders, genomic instability and cancer.** *Semin Cell Dev Biol* 2011, **2011**(22):875–885.
21. Ugur SA, Tolun A: **Homozygous WNT10b mutation and complex inheritance in Split-Hand/Foot Malformation.** *Hum Mol Genet* 2008, **17**:2644–2653.
22. Oort PJ, Warden CH, Baumann TK, Knotts TA, Adams SH: **Characterization of Tusc5, an adipocyte gene co-expressed in peripheral neurons.** *Mol Cell Endocrinol* 2007, **276**:24–35.
23. Manning JT, Scutt D, Wilson J, Lewis-Jones DI: **The ratio of 2nd to 4th digit length: a predictor of sperm numbers and concentrations of testosterone, luteinizing hormone and oestrogen.** *Hum Reprod* 1998, **13**:3000–3004.
24. Manning JT, Trivers RL, Singh D, Thornhill R: **The mystery of female beauty.** *Nature* 1999, **399**:214–215.
25. Williams TJ, Pepitone ME, Christensen SE, Cooke BM, Huberman AD, Breedlove NJ, Breedlove TJ, Jordan CL, Breedlove SM: **Finger-length ratios and sexual orientation.** *Nature* 2000, **404**:455–456.
26. Heald AH, Ivison F, Anderson SG, Cruickshank K, Laing I, Gibson JM: **Significant ethnic variation in total and free testosterone concentration.** *Clin Endocrinol* 2003, **58**:262–266.
27. Manning JT, Stewart A, Bundred PE, Trivers RL: **Sex and ethnic differences in 2nd to 4th digit ratio of children.** *Early Hum Dev* 2004, **80**:161–168.
28. Wang G, Vasquez KM: **Non-B DNA structure-induced genetic instability.** *Mutat Res* 2006, **598**:103–119.
29. Zhao J, Bacolla A, Wang G, Vasquez KM: **Non-B DNA structure-induced genetic instability and evolution.** *Cell Mol Life Sci* 2010, **67**:43–62.
30. Benko S, Gordon CT, Mallet D, Sreenivasan R, Thauvin-Robinet C, Brendehaug A, Thomas S, Bruland O, David M, Nicolino M, Labalme A, Sanlaville D, Callier P, Malan V, Huet F, Molven A, Dijoud F, Munnich A, Faivre L, Amiel J, Harley V, Houge G, Morel Y, Lyonnet S: **Disruption of a long distance regulatory region upstream of SOX9 in isolated disorders of sex development.** *J Med Genet* 2011, **48**:825–830.
31. Fraser FC: **Trinucleotide repeats not the only cause of anticipation.** *Lancet* 1997, **350**:459–460.

doi:10.1186/s13023-014-0125-5
Cite this article as: Nagata *et al.*: Japanese founder duplications/triplications involving *BHLHA9* are associated with split-hand/foot malformation with or without long bone deficiency and Gollop-Wolfgang complex. *Orphanet Journal of Rare Diseases* 2014 **9**:125.

CLINICAL REPORT

AMERICAN JOURNAL OF medical genetics PART A

De Novo Duplication of 17p13.1–p13.2 in a Patient With Intellectual Disability and Obesity

**Yukiko Kuroda,[1] Ikuko Ohashi,[1] Makiko Tominaga,[1] Toshiyuki Saito,[2] Jun-ichi Nagai,[2] Kazumi Ida,[1] Takuya Naruto,[1] Mitsuo Masuno,[3] and Kenji Kurosawa[1]*

[1]Division of Medical Genetics, Kanagawa Children's Medical Center, Yokohama, Japan

[2]Department of Clinical Laboratory, Kanagawa Children's Medical Center, Yokohama, Japan

[3]Genetic Counseling Program, Kawasaki University of Medical Welfare, Kurashiki, Japan

Manuscript Received: 5 September 2013; Manuscript Accepted: 8 January 2014

17p13.1 Deletion encompassing *TP53* has been described as a syndrome characterized by intellectual disability and dysmorphic features. Only one case with a 17p13.1 duplication encompassing *TP53* has been reported in a patient with intellectual disability, seizures, obesity, and diabetes mellitus. Here, we present a patient with a 17p13.1 duplication who exhibited obesity and intellectual disability, similar to the previous report. The 9-year-old proposita was referred for the evaluation of intellectual disability and obesity. She also exhibited insulin resistance and liver dysfunction. She had wide palpebral fissures, upturned nostrils, a long mandible, short and slender fingers, and skin hyperpigmentation. Array comparative genomic hybridization (array CGH) detected a 3.2 Mb duplication of 17p13.1–p13.2 encompassing *TP53*, *FXR2*, *NLGN2*, and *SLC2A4*, which encodes the insulin-responsive glucose transporter 4 (GLUT4) associated with insulin-stimulated glucose uptake in adipocytes and muscle. We suggest that 17p13.1 duplication may represent a clinically recognizable condition characterized partially by a characteristic facial phenotype, developmental delay, and obesity.

Key words: 17p13.1 duplication; *TP53*; *SLC2A4*; obesity; GLUT4

How to Cite this Article:
Kuroda Y, Ohashi I, Tominaga M, Saito T, Nagai J-I, Ida K, Naruto T, Masuno M, Kurosawa K. 2014. De novo duplication of 17p13.1–p13.2 in a patient with intellectual disability and obesity.
Am J Med Genet Part A 9999:1–5.

INTRODUCTION

Many copy number variations (CNVs) in specific loci are established as recognizable syndromes. For example, CNVs at 17p13.3, including *YWHAE* and *PAFAH1B1*, have been reported as 17p13.3 deletion syndrome with abnormal brain structure and 17p13.3 duplication syndrome with intellectual disability [Bruno et al., 2010]. A 17p13.1 deletion encompassing *TP53* was previously reported as a syndrome with intellectual disability and dysmorphic features, but without tumors [Krepischi-Santos et al., 2009; Schluth-Bolard et al., 2009; Shlien et al., 2010]. The germline *TP53* (MIM 191170) mutation causes Li–Fraumeni syndrome, also known as autosomal-dominant cancer-susceptibility condition. Genomic deletions of 17p13.1 encompassing *TP53* are associated with two distinct phenotypes, described as cancer-susceptibility and intellectual disability with dysmorphic features. CNVs in 17p13.1 arise by Alu-mediated nonallelic homologous recombination and share a common critical region with 17p13.1 deletion syndrome [Shlien et al., 2010]. Only one case with a 17p13.1 duplication encompassing *TP53* and characterized by intellectual disability, seizures, and obesity has been reported [Belligni et al., 2012]. The previous studies demonstrated the correlation between the deleted genes and phenotype in 17p13.1 deletion, but not 17p13.1 duplication. Here, we report a second patient with a 17p13.1 duplication who also exhibited intellectual disability and obesity.

CLINICAL REPORT

The proposita was the first child of healthy and nonconsanguineous parents. She was delivered at 40 weeks of gestation after an uneventful pregnancy. Her birth weight was 2,410 g (−2.1 SD), her length was 43.9 cm (−3.6 SD), and her occipital frontal circumference (OFC) was 30.3 cm (−2.3 SD). She had prenatal growth retardation. During infancy, hypotonia was noted, but her feeding

The authors have no conflicts of interest to declare.
Grant sponsor: The Ministry of Health, Labour and Welfare of Japan.
*Correspondence to:
Kenji Kurosawa, M.D., Ph.D., Division of Medical Genetics, Kanagawa Children's Medical Center, 2-138-4 Mutsukawa, Minami-ku, Yokohama 232-8555, Japan.
E-mail: kkurosawa@kcmc.jp
Article first published online in Wiley Online Library (wileyonlinelibrary.com): 00 Month 2014
DOI 10.1002/ajmg.a.36477

and growth were good. She started controlling her head at 4 months, sitting at 6 months, and walking unsupported at the age of 16 months. She was referred to our hospital at the age of 3 years for the assessment of developmental delay. A clinical examination revealed hypotonia. At the age of 4 years, her height was 97.3 cm (−1.6 SD), her weight was 16.9 kg (0.0 SD), and her OFC was 48.2 cm (−1.2 SD). She exhibited obesity at the age of 7 years, at which time her height was 114.0 cm (−1.0 SD), and her weight was 29.5 kg (+1.8 SD). She showed learning disability (IQ 50–58) and attended a special class at an elementary school. She was referred again to our hospital for the assessment of developmental delay and obesity at the age of 9 years. At this time, her height was 129.5 cm (−0.2 SD), her weight was 41.3 kg (+2.1 SD), and her OFC was 53.5 cm (+1.6 SD). Her body mass index (BMI) was 24.6. She also exhibited liver dysfunction and insulin resistance (AST 45 IU/L; AST 67 IU/L; IRI 617.4 μU/ml; glucose 159 mg/dl; HbA1c 5.3%; total cholesterol 172 mg/dl; triglyceride 112 mg/dl). Her thyroid function and adrenal hormone levels were normal. She had a coarse face appearance with wide palpebral fissures, upturned nostrils, and a long mandible (Fig. 1).

MATERIALS AND METHODS

Written informed consent was obtained from the parents of the patient in accordance with the Kanagawa Children's Medical Center Review Board and Ethics Committee.

Total genomic DNA was obtained from lymphocytes using standard techniques. Array comparative genomic hybridization (CGH) was performed using the Agilent SurePrint G3 Human CGH Microarray Kit 8 × 60 k (Agilent Technologies, Inc., Santa Clara, CA) according to the manufacturer's instructions. The results were analyzed using Agilent Genomic Workbench software.

A fluorescence in situ hybridization (FISH) analysis for determining the duplication of 17p13.1–p13.2 was performed using bacterial artificial chromosome (BAC) clones that were selected from the May 2004 (NCBI35/hg17) Assembly of the UCSC Genome Browser for the Human Genome (http://genome.ucsc.edu/). All DNAs were labeled using nick translation according to the manufacturer's instructions (Abbott-Vysis, Des Plains, IL). Hybridization, post-hybridization washing, and counterstaining were performed according to standard procedures. Slides were analyzed using a completely motorized epifluorescence microscope (Leica DMRXA2) equipped with a CCD camera. Both the camera and the microscope were controlled using Leica CW4000 M-FISH software (Leica Microsystems Imaging Solutions, Cambridge, UK) [Kurosawa et al., 2012].

RESULTS

A chromosome analysis revealed a normal female karyotype. Array CGH revealed an approximately 3.2 Mb duplication at 17p13.1–p13.2, extending from position 6,013,291 to 9,214,914 bp (GRCh37/hg19). FISH was performed with a test probe for the 17p13 duplicated region (RP11-199F11 chr17: 7,441,503–7,598,744) and a control probe for the centromere of chromosome 17 (Abbott-Vysis); a duplication was confirmed (Fig. 2). No duplication or translocation was present in her parents.

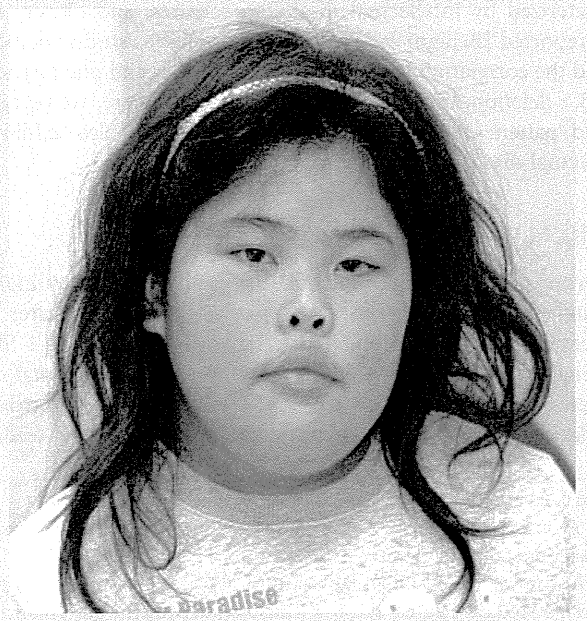

FIG. 1. A photograph of the patient at the age of 9 years. She had wide palpebral fissures, upturned nostrils, and a long mandible.

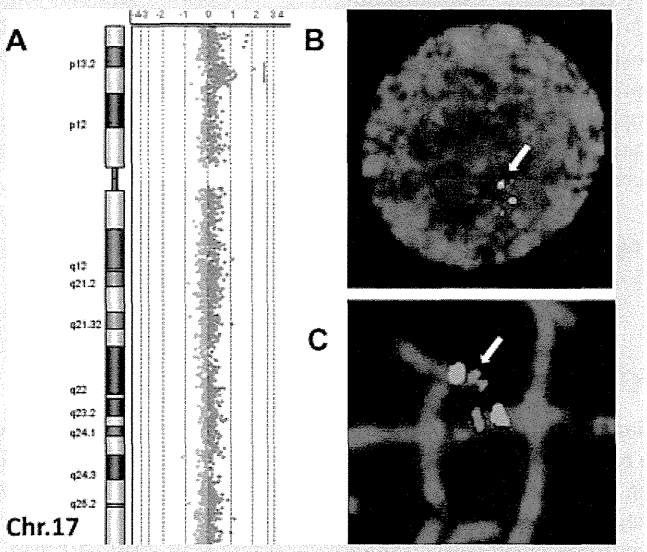

FIG. 2. Analysis of duplication at 17p13.1-p13.2. A: Array CGH showing the 3.2 Mb duplicated region at 17p13.1–p13.2. B: Interphase. C: Metaphase FISH in lymphocytes using the RP11-199F11 clone (chr17: 7,441,503–7,598,744) as a probe specific for 17p13.2 (red). The green signal shows the centromere region of chromosome 17 as a control. The patient has three signals, consistent with a duplication at 17p13.1–p13.2.

DISCUSSION

17p13.1 Duplication cases have been previously reported as exhibiting intellectual disability and multiple congenital anomalies [Belligni et al., 2012; Coutton et al., 2012]. The present case with a 17p13.1 duplication exhibited obesity and intellectual disability, similar to a previous report [Belligni et al., 2012]. Belligni et al. [2012] reported a case with a 17p13.1 duplication of 790–830 kb that exhibited moderate intellectual disability, seizures, obesity, insulin resistance, and hypertriglyceridemia. Eight patients with overlapping duplications have been reported in the DECIPHER database (Patients 4165, 250377, 258588, 262186, 256668, 250301, 258312, and 274634; Fig. 3). All the cases had intellectual disability, three of the eight cases had obesity, and four of the eight cases had seizures. Two patients with overlapping duplications have been reported in the ISCA database (nssv578737, nssv14955761). Both patients had intellectual disability but no other clinical data were available (Table I). Coutton et al. [2012] reported a case with discontinuous duplications at 17p13.1 consisting of 140 and 586 kb that did not encompass the *TP53* gene or the critical region for 17p13.1 deletion syndrome. The case exhibited mild intellectual disability, growth retardation, and an appearance similar to that of Silver–Russell syndrome. The other genes included by the discontinuous duplicated region may have affected the phenotype in a different manner from that in the presently reported patient and the case reported by Belligni et al. [2012].

There are several candidate genes for intellectual disability in the 17p13.1 duplicated region. Common overlapping duplicated region includes *DLG4* (disks large drosophila homolog 4; MIM 602887), *KCTD11* (potassium channel tetramerization domain containing protein 11; MIM 609848), *GPS2* (G protein pathway suppressor 2; MIM 601935), and *GABARAP* (GABA-A receptor associated protein like 1; MIM 607420). These genes are highly expressed in brain, so the region is previously suggested to candidates in 17p13.1 deletion [Komoike et al., 2010; Coutton et al., 2012]. Other duplicated region includes *FXR2* (MIM 605339) and *NLGN2* (MIM 606479). *FXR2* is highly expressed in the brain and codes the fragile X-related proteins 2, a homolog of the fragile X mental retardation gene (*FMR1*). *FMR1*, *FXR1*, and *FXR2* form a family characterized by functional similarities, such as RNA binding, polyribosomal association, and nucleocytoplasmic shuttling. *FXR2*-knockout mouse exhibited hyperactive behavior in an animal model [Bontekoe et al., 2002]. *NLGN2* encodes neuroligin-2, a site-specific ligand for beta-neurexins, and may be involved in synaptic signal transmission through interactions with neurexin family members. Mutations in neuroligin and neurexin family members (*NRXN1*, *NLGN3*, *NLGN4*) are associated with autism spectrum disorder [Jamain et al., 2003; Feng et al., 2006].

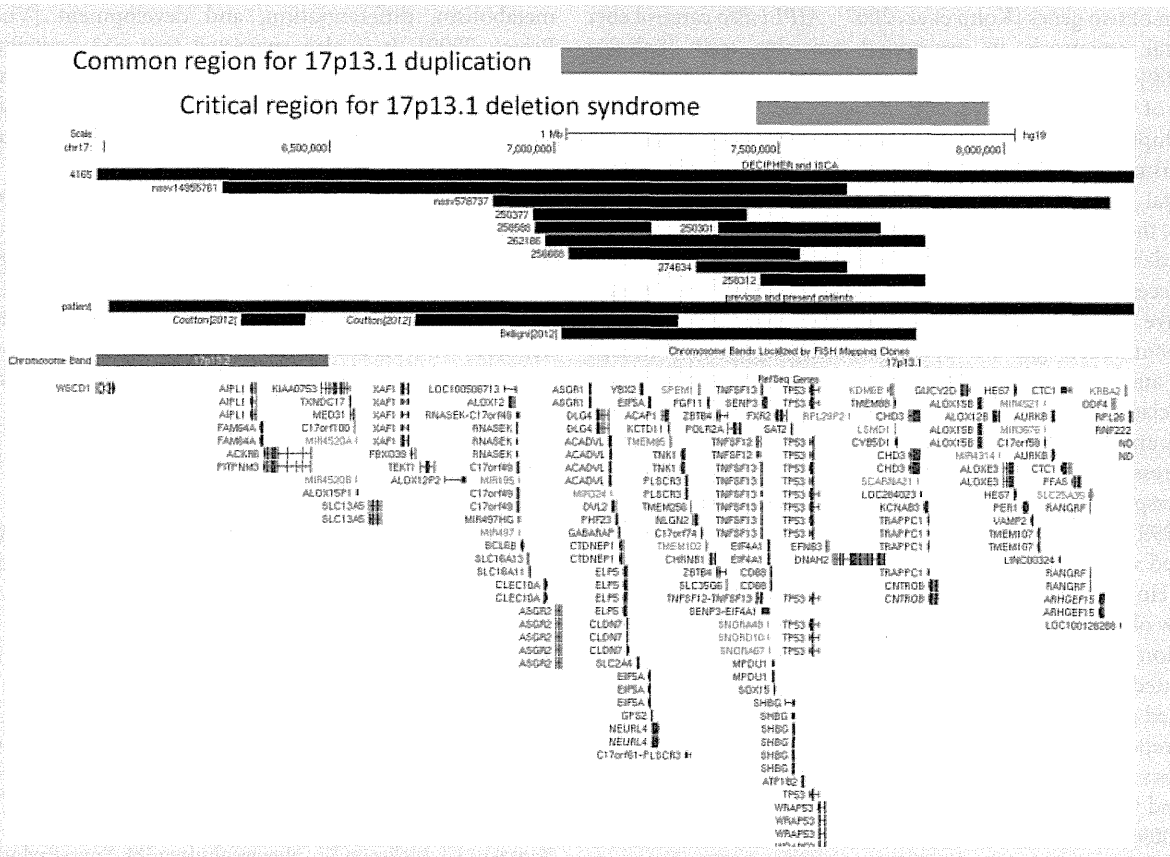

FIG. 3. Mapping of overlapping duplications in the patient and the previous reported cases and duplicated genes on chromosome 17p13.1–p13.2. Array data were uploaded into the UCSC genome browser, NCBI Build 37, February 2009, hg19 Assembly [http://www.genome.ucsc.edu].

TABLE I. Clinical Features of Patients With 17p13.1 Duplication

	Present case	Belligni et al. [2012]	Coutton et al. [2012]	DECIPHER 8 patients	ISCA 2 patients
Intellectual disability	+	+	+	8/8	2/2
Seizures	−	+	−	4/8	
Microcephaly	−	−	−	1/8	
Short stature	−	−	+	2/8	
Obesity	+	+	−	3/8	
Insulin resistance	+	+	−	1/8	
Hypothyroidism	−	+	−	1/8	
Other endocrinological dysfunction	Liver dysfunction	Hypertriglyceridemia	−	Hypogonadism [256668] Delayed skeletal maturation [4165]	
Others	Dysmorphic features	Astigmatism, Long mandible	Relative macrocephaly	Hypospadia [250377] Pulmonic stenosis [274634] 2/3 syndactyly [256668]	

The duplicated region of 17p13.2 contains two genes: *PITPNM3* (MIM 608921) and *AIPL1* (MIM 604392). Autosomal dominant type cone rod dystrophy has been reported in cases of heterozygous mutation of two genes [Kohn et al., 2007]. *AIPL1* also causes Leber congenital amaurosis in autosomal recessive trait [Sohocki et al., 2000]. Diseases have not been reported associated with dosage changes of these genes.

The duplicated region also contains three genes associated with metabolism: *MPDU1* (MIM 604041), the mutation of which causes congenital glycosylation disorder type 1f; and *ACADVL* (MIM 609575), the mutation of which causes very long-chain acyl-coenzyme A dehydrogenase deficiency. Both are associated with autosomal recessive disorder. *SLC2A4* (MIM 138190), the insulin-responsive glucose transporter 4 (GLUT4), plays a key role in insulin-stimulated glucose uptake in adipocytes and muscle [Huang and Czech, 2007]. Diabetes mellitus type 2 and obesity are associated with the impaired regulation of *SLC2A4* gene expression and function. Mice that were genetically engineered to overexpress the *SLC2A4* gene systematically exhibited enhanced insulin responsiveness and peripheral glucose utilization [Charron et al., 1999]. We assumed that *SLC2A4* overexpression might be associated with the increased uptake of glucose to adipocytes and obesity. However, the patient reported by Coutton et al. [2012] did not show obesity and growth retardation has not been reported in association with deletion of the *SLC2A4* gene. Obesity is possibly contributed to by not only *SLC2A4* overexpression but also other duplicated genes or genes not included in duplicated region of the patient reported by Coutton et al. [2012].

Tumors have not been observed in patients with 17p13.1 deletions and duplications encompassing *TP53* [Krepischi-Santos et al., 2009; Schluth-Bolard et al., 2009; Shlien et al., 2010]. The p53 protein acts as a tumor suppressor and plays an important role in controlling of a cell cycle and maintaining the integrity of the genome [Ullrich et al., 1992]. Tumors were shown in patients with mutations and partial small deletion of the *TP53* gene but not large genomic deletions. There is no evidence of the correlation between dosage change of the *TP53* and cancer predisposition. The p53 roles in normal cellular processes have recently been reported in energy metabolism, differentiation, and development [Vousden and Prives, 2009]. It is also suggested that p53 contributes to the pathology of various neurodegenerative diseases [Bretaud et al., 2007; Leandro et al., 2013]. Abnormal expression levels of TP53 might result to affect the development and maintenance of the central nerve system.

In conclusion, 17p13.1 duplication appears to exhibit common features characterized by intellectual disability and multiple congenital anomalies. The present and previously reported cases of 17p13.1 duplication do not share common breakpoints, but they do have a common region consistent with the critical region of 17p13.1 deletion syndrome. Our case suggests that 17p13.1 duplication syndrome is characterized by intellectual disability and obesity.

ACKNOWLEDGMENTS

This research was supported in part by a Grant-in-aid from the Ministry of Health, Labour and Welfare, Japan. We thank the patient and the patient's family for their cooperation.

REFERENCES

Belligni EF, Di Gregorio E, Biamino E, Calcia A, Molinatto C, Talarico F, Ferrero GB, Brusco A, Silengo MC. 2012. 790 Kb microduplication in chromosome band 17p13.1 associated with intellectual disability, afebrile seizures, dysmorphic features, diabetes, and hypothyroidism. Eur J Med Genet 55:222–224.

Bontekoe CJ, Mcllwain KL, Nieuwenhuizen IM, Yuva-Paylor LA, Nellis A, Willemsen R, Fang Z, Kirkpatrick L, Bakker CE, McAninch R, Cheng NC, Merriweather M, Hoogeveen AT, Nelson D, Paylor R, Oostra BA. 2002. Knockout mouse model for Fxr2: A model for mental retardation. Hum Mol Genet 11:487–498.

Bretaud S, Allen C, Ingham PW, Bandmann O. 2007. p53-dependent neuronal cell death in a DJ-1-deficient zebrafish model of Parkinson's disease. J Neurochem 100:1626–1635.

Bruno DL, Anderlid BM, Lindstrand A, van Ravenswaaij-Arts C, Ganesamoorthy D, Lundin J, Martin CL, Douglas J, Nowak C, Adam MP, Kooy RF, Van der Aa N, Reyniers E, Vandeweyer G, Stolte-Dijkstra I, Dijkhuizen T, Yeung A, Delatycki M, Borgström B, Thelin L, Cardoso C, van Bon B, Pfundt R, de Vries BB, Wallin A, Amor DJ, James PA, Slater HR, Schoumans J. 2010. Further molecular and clinical delineation of co-locating 17p13.3 microdeletions and microduplications that show distinctive phenotypes. J Med Genet 47:299–311.

Charron MJ, Katz EB, Olson AL. 1999. GLUT4 gene regulation and manipulation. J Biol Chem 274:3253–3256.

Coutton C, Devillard F, Vieville G, Amblard F, Lopez G, Jouk P-S, Satre V. 2012. 17p13.1 microduplication in a boy with Silver–Russell syndrome features and intellectual disability. Am J Med Genet Part A 158A:2564–2570.

Feng J, Schroer R, Yan J, Song W, Yang C, Bockholt A, Cook EH Jr, Skinner C, Schwartz CE. 2006. High frequency of neurexin 1 beta signal peptide structural variants in patients with autism. Neurosci Lett 409:10–13.

Huang S, Czech MP. 2007. The GLUT4 glucose transporter. Cell Metab 5:237–252.

Jamain S, Quach H, Betancur C, Rastam M, Colineaux C, Gillberg IC, Soderstrom H, Giros B, Leboyer M, Gillberg C, Bourgeron T, Paris Autism International Sibpair Study. 2003. Mutations of the X-linked genes encoding neuroligins NLGN3 and NLGN4 are associated with autism. Nat Genet 34:27–29.

Kohn L, Kadzhaev K, Burstedt MSI, Haraldsson S, Hallberg B, Sandgren O, Golovleva I. 2007. Mutation in the PYK2-binding domain of PITPNM3 causes autosomal dominant cone dystrophy (CORD5) in two Swedish families. Eur J Hum Genet 15:664–671.

Komoike Y, Shimojima K, Liang JS, Fujii H, Maegaki Y, Osawa M, Fujii S, Higashinakagawa T, Yamamoto T. 2010. A functional analysis of GABARAP on 17p13.1 by knockdown zebrafish. J Hum Genet 55:155–162.

Krepischi-Santos ACV, Rajan D, Temple IK, Shrubb V, Crolla JA, Huang S, Beal S, Otto PA, Carter NP, Vianna-Morgante AM, Rosenberg C. 2009. Constitutional haploinsufficiency of tumor suppressor genes in mentally retarded patients with microdeletions in 17p13.1. Cytogenet Genome Res 125:1–7.

Kurosawa K, Tanoshima-Takei M, Yamamoto T, Ishikawa H, Masuno M, Tanaka Y, Yamanaka M. 2012. Sirenomelia with a de novo balanced translocation 46,X,t(X;16)(p11.23:p12.3). Congenit Anom (Kyoto) 52:106–110.

Leandro GS, Lobo RR, Oliveira DVNP, Moriguti JC, Sakamoto-Hojo ET. 2013. Lymphocytes of patients with Alzheimer's disease display different DNA damage repair kinetics and expression profiles of DNA repair and stress response genes. Int J Mol Sci 14:12380–12400.

Schluth-Bolard C, Sanlaville D, Labalme A, Till M, Morin I, Touraine R, Edery P. 2009. 17p13.1 microdeletion involving the TP53 gene in a boy presenting with mental retardation but no tumor. Am J Med Genet Part A 152A:1278–1282.

Shlien A, Baskin B, Achatz MIW, Stavropoulos DJ, Nichols KE, Hudgins L, Morel CF, Adam MP, Zhukova N, Rotin L, Novokmet A, Druker H, Shago M, Ray P, Hainaut P, Malkin D. 2010. A common molecular mechanism underlies two phenotypically distinct 17p13.1 microdeletion syndromes. Am J Hum Genet 87:631–642.

Sohocki MM, Bowne SJ, Sullivan LS, Blackshaw S, Cepko CL, Payne AM, Bhattacharya SS, Khaliq S, Mehdi SQ, Birch DG, Harrison WR, Elder FFB, Heckenlively JR, Daiger SP. 2000. Mutations in a new photoreceptor-pineal gene on 17p cause Leber congenital amaurosis. Nature Genet 24:79–83.

Ullrich SJ, Anderson CW, Mercer WE, Appella E. 1992. The p53 tumor suppressor protein, a modulator of cell proliferation. J Biol Chem 267:15259–15262.

Vousden KH, Prives C. 2009. Blinded by the light: The growing complexity of p53. Cell 137:413–431.

RESEARCH ARTICLE

AMERICAN JOURNAL OF medical genetics PART A

Early Manifestations of BPAN in a Pediatric Patient

Nobuhiko Okamoto,[1]* Tae Ikeda,[2] Tatsuji Hasegawa,[3] Yuto Yamamoto,[1] Kazumi Kawato,[1] Tomohiro Komoto,[4,5] and Issei Imoto[5]

[1]Department of Medical Genetics, Osaka Medical Center and Research Institute for Maternal and Child Health, Osaka, Japan

[2]Department of Pediatric Neurology, Osaka Medical Center and Research Institute for Maternal and Child Health, Osaka, Japan

[3]Department of Pediatrics, Maizuru Medical Center, Maizuru, Japan

[4]Student Lab, The University of Tokushima Faculty of Medicine, Tokushima, Japan

[5]Department of Human Genetics, Institute of Health Biosciences, The University of Tokushima Graduate School, Tokushima, Japan

Manuscript Received: 23 May 2014; Manuscript Accepted: 14 August 2014

Neurodegeneration with brain iron accumulation (NBIA) comprises a clinically and genetically heterogeneous group of progressive brain disorders with several distinguishable subtypes. Recently, *WDR45* mutations were reported in patients with β-propeller protein-associated neurodegeneration (BPAN), characterized by early intellectual disability followed by delayed progressive motor and cognitive deterioration with onset in the second to third decade. BPAN has a distinct brain magnetic resonance imaging (MRI) pattern showing iron deposition in the globus pallidus and substantia nigra. To date, many of the BPAN patients have been diagnosed in adulthood. Here, we report on 6-year-old girl with BPAN diagnosed by whole exome sequencing. She showed Rett syndrome-like manifestations, a peculiar facial appearance and mildly elevated serum enzymes. Brain iron accumulation was detected by T2*-weighted MRI and T2-star weighted angiography (SWAN). This unique combination of clinical and neuroimaging features may be helpful for early diagnosis of BPAN. © 2014 Wiley Periodicals, Inc.

Key words: BPAN; Rett syndrome; *WDR45*, whole exome sequencing

How to Cite this Article:
Okamoto N, Ikeda T, Hasegawa T, Yamamoto Y, Kawato K, Komoto T, Imoto I. 2014. Early manifestations of BPAN in a pediatric patient.
Am J Med Genet Part A. 9999:1–5.

INTRODUCTION

Neurodegeneration with brain iron accumulation (NBIA) is a heterogeneous progressive brain disorder presenting with neurological and psychiatric symptoms with multiple recognizable genetic subtypes. Most of these subtypes are inherited in an autosomal recessive manner. Haack et al. [2012] and Saitsu et al. [2013] revealed mutations of *WDR45* located in Xp11.23 in patients with Static Encephalopathy of childhood with Neurodegeneration in Adulthood (SENDA), which is also referred to as NBIA5 or more appropriately as β-propeller protein-associated neurodegeneration (BPAN). *WDR45* encodes a protein associated with autophagy, a cellular process that degrades damaged organelles or protein aggregation. Autophagy is involved in many pathological processes, including neurodegenerative disorders.

BPAN is essentially static, with slow motor and cognitive gains until adolescence or early adulthood. Hayflick et al. [2013] reviewed 23 mutation-positive subjects (20 females). They reported that the natural history of BPAN was markedly uniform: global developmental delay in childhood and further regression in early adulthood with progressive dystonia, Parkinsonism and dementia resulting in severe disability. Seizures, spasticity and disordered sleep are common features. Brain magnetic resonance imaging (MRI) shows iron accumulation in the globus pallidus (GP) and substantia nigra (SN). A characteristic finding is T1-weighted hyperintensity surrounding a central band of hypointensity ("halo") in the SN. Cerebral and cerebellar atrophy are also observed. Verhoeven et al. [2014] described with respect to course and neurological as well as neuropsychiatric phenotypes of BPAN.

Here, we report on a pediatric patient with BPAN diagnosed by next generation sequencing.

CLINICAL REPORT

The 6-year-old Japanese girl was the second child of healthy and nonconsanguineous parents. She was born at 40 weeks of gestation

Conflict of interest: The authors report no conflicts of interest.
Grant sponsor: Ministry of Health, Labour and Welfare, Japan.
*Correspondence to:
Dr. Nobuhiko Okamoto, Department of Medical Genetics, Osaka Medical Center and Research Institute for Maternal and Child Health 840, Murodo-cho, Izumi, Osaka 594-1101, Japan.
E-mail: okamoto@osaka.email.ne.jp
Article first published online in Wiley Online Library (wileyonlinelibrary.com): 00 Month 2014
DOI 10.1002/ajmg.a.36779